Chemical, Energetic, and Structural Characteristics of Hydrothermal Carbonization Solid Products for Lawn Grass

Shuqing Guo,* Xiangyuan Dong, Kaituo Liu, Hailong Yu, and Caixia Zhu

Hydrothermal carbonization (HTC) of lawn grass was carried out at 200 °C and 240 °C for 30 to 180 min. The chemical, energetic, and structural characteristics of HTC solid residues were investigated. Results from HTC experiments indicate that solid mass yield of all solid residues was 31 to 50%. The hydrogen/carbon (H/C) and oxygen/carbon (O/C) atomic ratios of all solid residues were 1.17 to 1.64 and 0.45 to 0.65, respectively. The higher heating value (HHV) increased up to 20.54 MJ/kg with increasing HTC residence time at 240 °C for 180 min. Both XRD patterns and FTIR spectra show that differences occur with samples treated as compared to the raw material. Solid hydrochar exhibited higher ordered structure characteristics and was mainly derived from amorphous components degradation when the residence time was increased from 30 to 180 min at 200 °C, while hydrochar formed from cellulose components degradation with increased residence time at 240 °C. According to the results studied, it was found that prolonged residence time was favorable to the formation of hydrochar from lawn grass.

INTRODUCTION

In recent years, there has been increasing concern regarding the energy shortage and environmental issues arising from fossil fuel. Biomass is regarded as an alternative energy source due to its wide availability, renewability, and cleanness. However, effective treatment and conversion of biomass into energy requires additional research. To date, varieties of techniques have been applied in biomass treatment and conversion, such as combustion, pyrolysis, gasification (Yang *et al.* 2006; Wiedner *et al.* 2013; Chen *et al.* 2014). However, a complicated high temperature process for biofuels and bioproducts will undesirably be accompanied by a high cost.

In recent years, hydrothermal carbonization (HTC) has been paid considerable attention for biomass treatment (Funke and Ziegler 2010). Hydrothermal carbonization is a wet thermal conversion technique that is simple, cheap, and easy to perform with a mild reaction condition (180 to 250 °C) as compared to other techniques (Funke and Ziegler 2010). The biomass should be submerged to ensure that the hydrothermal reaction occurred during the whole reaction process. The final solid products of HTC are often called hydrochar. Hydrochar has been regarded potentially useful as a soil additive, for carbon sequestration, adsorbents, container nurseries, and even for fuels. (Steinbeiss *et al.* 2009; Roman *et al.* 2012; Wiedner *et al.* 2013). In recent years, considerable HTC

research has been conducted on methods for obtaining hydrochar. Roman *et al.* (2012) studied walnut shell and sunflower stem by HTC, and found that coalification was promoted by increasing the calorific value of the solid hydrochar. Xiao *et al.* (2012) treated corn stalk and *Tamarix ramosissima* by HTC, revealing that the solid products mainly consisted of lignin with a high degree of aromatization and a large amount of oxygen-containing groups. Moreover, the hydrochar had a considerably higher heating value (HHV) than that of the raw material. Poerschmann *et al.* (2014) utilized wet biomass, brewer's spent grain, to produce biocoal. Their experimental results showed that the energy densification of biocoals was increased compared to the raw material. The HHV data for HTC coals was similar to that of lignite. Gao *et al.* (2013) studied the chemical and structural properties of water hyacinth hydrochar with increasing time. They found that higher HHV and better structural characterization of hydrochar could be obtained with increased time. These studies on HTC indicated that the physicochemical characteristics of hydrochar were dependent on the property of feedstock. In addition, the process parameters such as reaction temperature and time had a significant effect on the HTC process (Funke and Ziegler 2010; Lu and Pellechia 2013; Gao *et al* 2013; Zhang *et al.* 2015). Biomass could undergo complicated chemical reactions under different process conditions including hydrolysis, dehydration, decarboxylation, and condensation polymerization during hydrothermal carbonization (Funke and Ziegler 2010; Sevilla *et al.* 2011; Kang *et al.* 2012). To understand the hydrothermal carbonization process for different types of feedstock under various reaction conditions, fundamental research on HTC still has further to go.

Grass is a class of biomass easily found in urban areas, and was reported previously to produce value added products such as activated carbon (Kalyani *et al.* 2013), nitrogen-doped carbon materials (Liu *et al.* 2012), and biogas (McEniry *et al.* 2014; Meyer *et al.* 2014). However, few studies have been done that provide valuable information regarding the characteristics of hydrochar from HTC lawn grass at different residence times. To achieve deeper insight into the influence of residence time on HTC process of lawn grass, the HTC experiments of lawn grass changing residence time at two reaction temperatures were carried out. To characterize the evolutions of hydrochar at different residence times, elemental analysis, X-ray diffraction (XRD), and Fourier transform infrared (FTIR) spectroscopy were used to study the chemical, energetic, and structural characteristics of lawn grass hydrochar.

EXPERIMENTAL

Materials

Lawn grass used in this study was collected from the Zhengzhou urban area. The grass was dried by natural air for a few days, and then broken into 1- to 2-mm samples. The raw samples were sealed in a plastic container for further use. The lignocellulosic compositions (%) of the dried samples were analyzed by the Van Soest analysis method (Zhang 2003). Elemental analysis of the samples was conducted on an element analyzer (EA3000, EuroVector, Italy). Proximate analyses of dried samples were determined according to the standard GB/T 28731 (2012). The test results were shown in Table 1. Lawn grass contained high cellulose, hemicellulose contents, and low lignin content. Elemental analysis indicated that the feedstock was mainly composed of C and O. Proximate analysis presented a high volatile matter content of 79.89%.

Table 1. Composition, Ultimate Analysis, and Proximate Analysis of Lawn Grass

Lignocellulosic composition (%)			Elemental analysis (Wt.%, db)					Proximate analysis (Wt.% , adb)			
Cellulose	Hemi cellulose	Lignin	C	H	N	S	O*	A	FC	V	M
41.7	35.8	8.02	42.85	7.25	2.68	0.00	43.37	3.72	13.11	79.89	3.28
*O was determined by difference; A: ash; FC: fixed carbon; V: volatile matters; M: moisture content; db: dry basis; adb: air dried basis											

Methods

The hydrothermal experiment was carried out in a 2-L, 316 L stainless steel autoclave, and its maximum temperature and pressure were 350 ºC and 22 MPa, respectively. The autoclave was heated by an electrical heater. To evenly heat the feedstock, the autoclave was equipped with a magnetic stirrer, and a maximum stirring speed was 1000 rpm. The hydrothermal processes were shown as following: first, 10 g of raw material and 300 mL of water were mixed and stirred evenly in the autoclave. Then, the autoclave was heated to 200 °C and 240 °C, respectively, then maintained for a desired residence time (30, 60, 90, 120, or 180 min). During the whole process, it was stirred at a speed of 200 rpm. After each residence time, the reactor was cooled to room temperature. The solid reaction product was collected by filtration, and then dried at 105 °C until a constant weight was achieved. The dried samples were then sealed in plastic container for further analysis.

The X-ray diffraction (XRD) patterns of the dried raw material and hydrothermally treated samples were measured using an X-ray analyzer (X'Pert PRO, PANalytical, Netherlands). The XRD spectra were obtained with a Cu target using kα radiation (λ = 0.1542 nm) generated from a 40-kV potential and 40-mA current. Intensities ranged from 5 to 50° with a 2 °/min continuous scan speed, and the scan step size was 0.03°. The chemical structure and characteristics of the dried samples functional groups were studied by Fourier transform infrared (FTIR) spectroscopy (Bruker Tensor 27, Bruker Optics, Germany). The IR spectra recorded varying wave number over the range of 400 to 4000 cm^{-1}, with a resolution of 4 cm^{-1} and scanning speed of 32 mm/s.

RESULTS AND DISCUSSION

Chemical and Energetic Characteristics

To evaluate the chemical and energetic characteristics of the dried samples, six equations, including those for solid mass yield (SY); C, H, and O fraction; normalized C, H, and O content; higher heating value (HHV); energy densification (ED); and energy retention efficiency (ERE) were defined as follows:

$$\text{Solid mass yield}(\%) = \frac{\text{mass of dried HTC solids}}{\text{mass of dried raw material}} \times 100\% \tag{1}$$

$$\text{C, H, O fraction}(\%) = \frac{\text{mass of C, H, O in dried HTC solids}}{\text{mass of C, H, O in dried raw material}} \times 100\% \tag{2}$$

$$\text{Normalized C, H, O content(\%)} = \frac{\text{mass of C, H, O in dried HTC solids}}{\text{mass of dried raw material}} \times 100\% \quad (3)$$

$$HHV(MJ/kg) = 0.3383 \times C + 1.422 \times (H\text{-}O/8) \quad (4)$$

$$\text{Energy densification} = \frac{HHV \text{ of dried HTC solids}}{HHV \text{ of dried raw material}} \quad (5)$$

$$\text{Energy retention efficiency(\%)} = \text{Solid mass yield} \times \text{Energy densification} \times 100\% \quad (6)$$

Solid mass yield is one of the key characteristics for HTC solid products. Figure 1 shows that the HTC solid mass yields *vs.* the residence time increased from 30 min to 180 min at 200 and 240 ºC.

(a) Solid mass yield
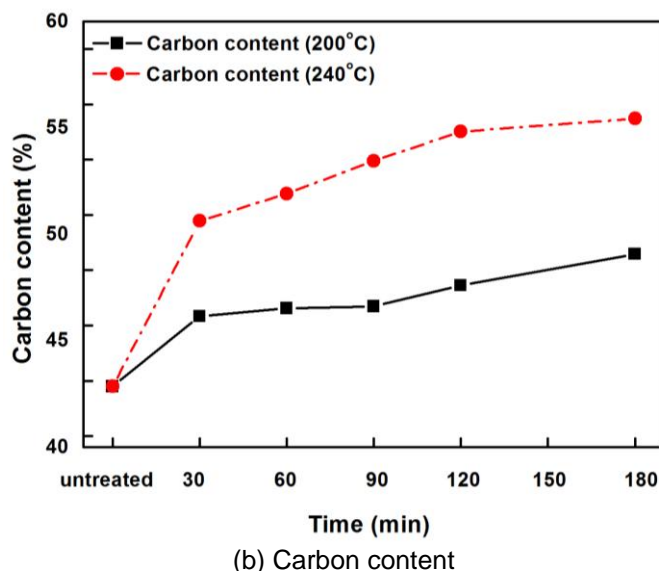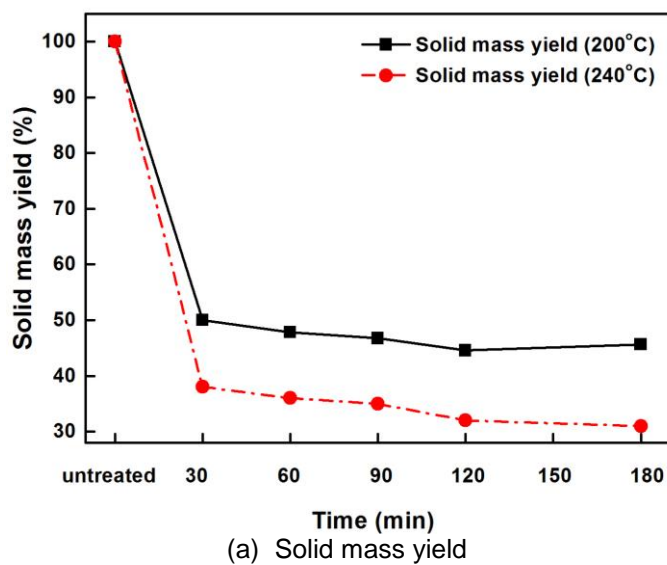
(b) Carbon content

Fig. 1. Solid mass yield and carbon content for feedstock and hydrochar at 200 and 240 °C

It can be observed that with 30 min of HTC treatment, the solid mass yield sharply decreased to 50% (200 ℃) and 38% (240 ℃) because part of the raw material (*i.e.*, hemicellulose, lignin, and cellulose) was hydrolyzed and solubilized into water or partitioned to gas and liquid phases (Bobleter 1994; Funke and Ziegler 2010). With increasing residence time from 30 to 180 min, the solid mass yield slowly decreased from 50 to 46% at 200 ℃, and from 38 to 31% at 240 ℃. The influence of the residence time on yield at both temperatures was similar and led to a slow decrease. However, the yield of hydrochar at 240 ℃ with residence time ranging from 30 min to 180 min was lower than those of all hydrochar at 200 ℃. This is because the HTC reaction of lignocellulosic biomass was a relatively slow process, and the reaction rate was mainly governed by temperature (Funke and Ziegler 2010). The amorphous hemicellulose degradation process was almost completed at 200 ℃. Meanwhile, the dissolved solid phase deposits (Reza *et al.* 2013) or polymerizes to form water insoluble polymer (Bobleter 1994; Funke and Ziegler 2010), which makes the solid product yield slowly decrease and level off as the residence time is increased. Meanwhile the cellulose slowly degraded at 240 ℃ (Funke and Ziegler 2010), which led to a lower yield of hydrochar.

The elemental composition of the samples can provide further insight into the chemical transformations of the samples. Carbon content for the untreated sample and HTC solid residues at 200 and 240 °C are shown in Fig. 1. It can be seen that the carbon content underwent a gradual increase. First, carbon content increased from 42.9 (untreated) to 46.15% (30 min treated at 200 °C) and to 50.63% (30 min treated at 240 °C), then a further increase to 49.1% (180 min treated at 200 °C) and to 55.43% (180 min treated at 240 °C), respectively. Figure 2 illustrates the C, H, and O fractions, which are the ratios of the mass of C, H, and O in the dried recovered solids to the corresponding mass of C, H, and O in the dried raw material.
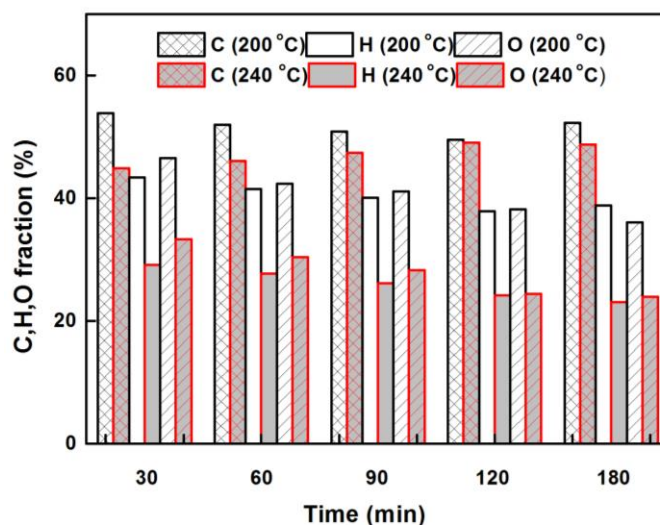
Fig. 2. C, H, and O fraction for hydrochar at 200 and 240 °C

After 30 min HTC treatment, C, H, and O fractions sharply decreased to 53.85%, 43.4%, and 46.5% at 200 °C, and to 44.89%, 29.07%, and 33.27% at 240 °C, respectively. This indicates that nearly or over half of the C, H, and O mass in dried raw sample were lost, which was mainly due to the solubilization or partition to gas and liquid phases. With an increasing residence time, the O and H fraction decreased to 36% and

37.8% at 200 °C, and to 23.59% and 23.07% at 240 °C, respectively. However, the C fraction at both temperatures showed less significant difference with residence time increased. This indicates that the increase of the carbon content with increasing residence time at each temperature (Fig. 1) was a result of the decrease in the H and O mass loss. The change trend for C fraction with increasing the residence time may be a combination result of hemicellulose and cellulose degradation and deposition of dissolved compounds. Additionally, the H and O fraction at 240 °C became obviously lower than that observed at 200 °C. The results indicated dehydration and decarboxylation reaction during lawn grass HTC were also significantly influenced by temperature. The changes of the C, H, and O fraction coincided with the changes of solid mass yield with increased time at both temperatures.

Figure 3 illustrates the normalized C, H, and O contents, which was calculated by the mass of C, H, and O in the recovered solids divided by the mass of the dried initial feedstock. From Fig. 3, it can be seen that after 30 min of HTC treatment, the normalized C mass decreased from 42.85 to 23.08% at 200 °C, to 19.24% at 240 °C. However, no substantial change about the normalized C mass was observed with a further increase in the residence time at both experimental temperatures. A similar trend in normalized mass of H was observed. Normalized O mass first decreased from 43.37 to 20.16% at 200 °C and 14.47% at 240 °C, and then further decreased to 15.6% at 200 °C and 10.26% at 240 °C with increasing the residence time. These results show that after 30 min of HTC treatment, the decrease of the solid mass yield was caused by the mass loss of C, H, and O. Since C and H mass changed mildly with increasing residence time, it can be concluded that the solid mass yield decrease is mainly due to the O loss. This result is consistent with other literature (Reza *et al.* 2013). Therefore, some organic acid (*e.g.* levulinic acid and formic acid) were formed and dissolved into liquid and a small amount of CO_2 released (Funke and Ziegler 2010; Reza *et al.* 2013). It is notable that the normalized C, H, and O contents at 240 °C were lower than those at 200 °C, which indicated the increased temperature promoted the chemical reaction.
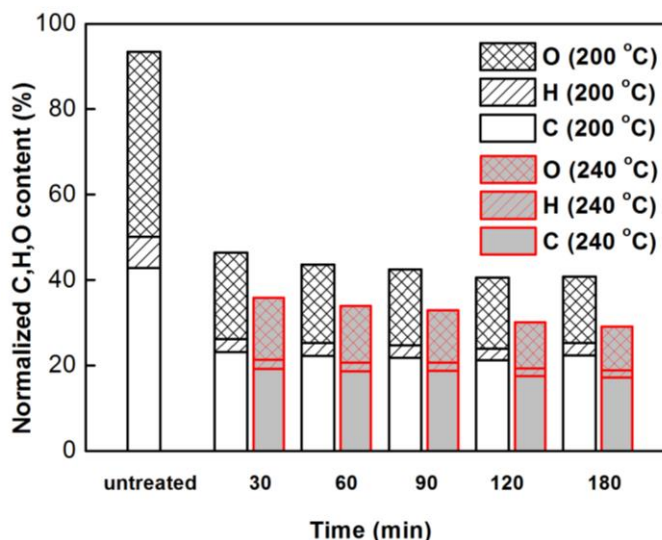
Fig. 3. Normalized C, H, and O content for feedstock and hydrochar at 200 and 240 °C

Higher heating value (HHV, as defined in Eq. 5), and the atomic H/C and O/C were calculated based on elemental content. Their relationship with time is presented in

Fig. 4. As expected, HHV increased from 17 (untreated) to 17.4 MJ/kg (30 min treated at 200 °C) and 18.24 MJ/kg (30 min treated at 240 °C). With increasing residence time, HHV reached 19.3 MJ/kg at 200 °C for 180 min, while, it achieved 20.54 MJ/kg at 240 °C for 180 min. This is because of the removal of low HHV components such as fragrances, oils, and hemicellulose at 200 °C and degradation and conversion of cellulose at 240 °C (Funke and Ziegler 2010; Reza *et al.* 2013). In contrast to HHV, H/C and O/C decreased as residence time increased. After HTC treatment, the H/C and O/C ratios were between 1.17 to 1.64 and 0.45 to 0.65 at 200 °C and 240 °C, respectively; this result is in accordance with a previous report (Wiedner *et al.* 2013). The high O/C ratio (0.4 to 0.6) may also indicate the presence of hydroxyl, carboxyl, and carbonyl groups (Wiedner *et al.* 2013). As shown in Fig. 4, the dehydration and decarboxylation pathways were marked. The reduction in H/C and O/C ratios followed these pathways. This indicates that dehydration and decarboxylation occurred during the HTC process as residence time and temperature were increasing (Funke and Ziegler 2010; Reza *et al.* 2014).
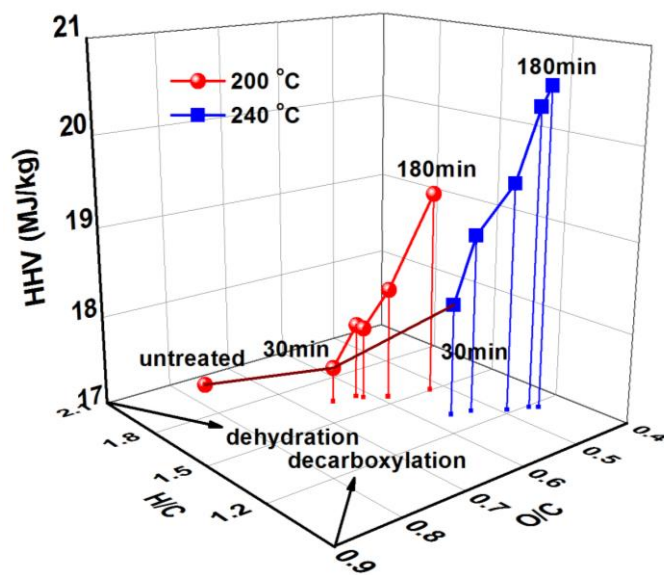
Fig. 4. HHV and Van Krevelen diagram of feedstock and hydrochar at 200 and 240 °C
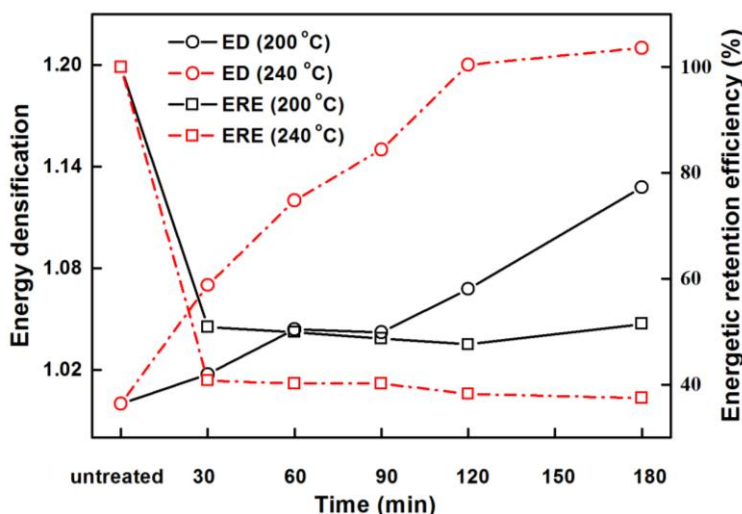
Fig. 5. Energy densification and energetic retention efficiency for feedstock and hydrochar at 200 and 240 °C

Energy densification and energy retention efficiency are shown in Fig. 5. As can be seen, energy densification presented a gradual increase, which was similar to that of carbon content. It first increased from 1 (untreated sample) to 1.02 (30 min treated sample), and then further increased to 1.13 (180 min treated) at 200 °C. It increased from 1.07 to 1.21 over the range of residence time at 240 °C. Energy retention efficiency followed a similar trend with solid mass yield, which exhibited a tendency of slight decrease. When compared with that from 200 °C, the hydrochar from 240 °C showed higher ED and lower ERE.

Structural Characteristics

The XRD patterns of untreated and hydrothermal treated samples are shown in Fig. 6. It can be seen that the XRD diffraction peaks for the untreated sample were broad, which suggest that the untreated samples have disordered and amorphous structures. After 30 min of 200 °C HTC treatment, the XRD pattern peaked at 2θ values of 15-20º and 22.7° and was sharper than those of the untreated materials. At the same time, a weaker peak appeared at a 2θ value of 34º. As stated in the literature (Hashaikeh *et al.* 2007), all three diffraction peaks represented the microcrystalline cellulose structure. This indicates that the amorphous component of the lawn grass (mostly hemicellulose) was removed. With increasing residence time at 200 °C, the XRD diffraction peaks for 2θ values of 15 to 20°, 22.7º, and 34° became sharper, but the changes were with a small difference. This suggests that the effect of residence time on HTC process was slow under the operating conditions (200 °C, 30 to 180 min). However, the hydrochar at 240 °C for 30 min showed a stronger peak at the three aforementioned diffraction angles. With the increase of residence time at 240 °C, XRD peaks corresponding to microcrystalline cellulose slowly declined, which indicated that the cellulose components began to degrade to form hydrochar and the structure of hydrochar had been changed.

For an in-depth analysis of the chemical variation of hydrochar with increasing time, the correlation between the crystallinity index and carbon content, oxygen content are presented in Fig.7 (a) and (b). Crystallinity index was calculated by the ratio of the difference between maximum 002 diffraction intensity at 2θ equal to 22.7º and the amorphous diffraction intensity at 2θ of 18º to maximum 002 diffraction intensity, which reflected the relative amount of crystalline cellulose in the total biomass (Li *et al.* 2011). Different trends in carbon and oxygen content changes with crystallinity index variations were observed at 200 and 240 °C. All P values (shown in Fig. 7) of fitting curves were less than 0.01, which showed that a highly significant correlation existed between carbon (oxygen) content and crystallinity index. At 200 °C, with time increasing, crystallinity index increased with increase of carbon content and decrease of oxygen content. However, a significant increase in crystallinity index was observed at 240 °C for 30 min (the highest black square point in Fig.7), and then an obvious decrease of crystallinity index was exhibited with variations of carbon and oxygen content as time increasing. This suggested that the feedstock solubilization and hydrochar formation at 200 °C mainly caused by amorphous components degradation. However, at 240 °C, hydrochar production followed by cellulose degradation and carbonization, which was characterized by significant declining of crystallinity index at times exceeding 30 min. Figure 7 distinctly shows the different pathways of carbonization with time variations at different temperatures, and it is particularly useful to understand hydrochar production during HTC. These results could further demonstrate the results of yield and elemental composition.

(a) 200 °C (b) 240 °C
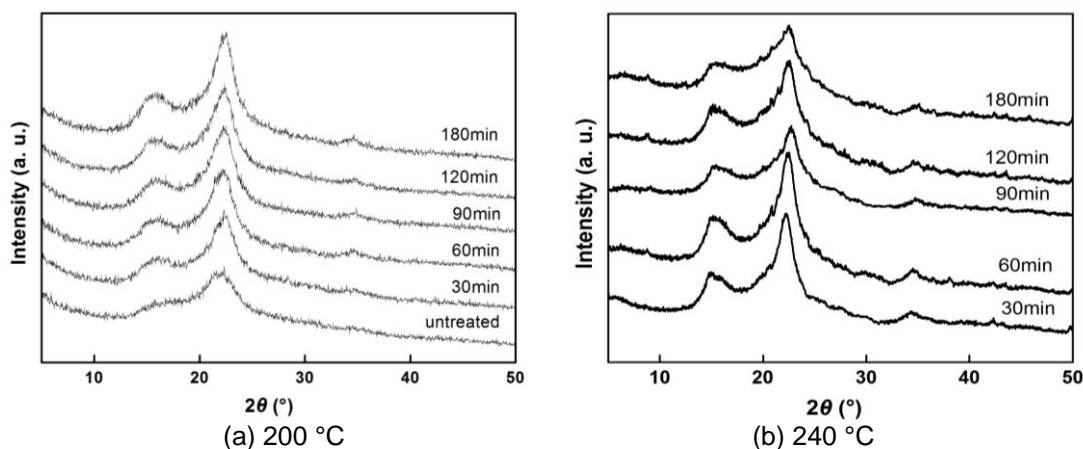
Fig. 6. X-ray diffraction pattern of feedstock and hydrochar at 200 and 240 °C
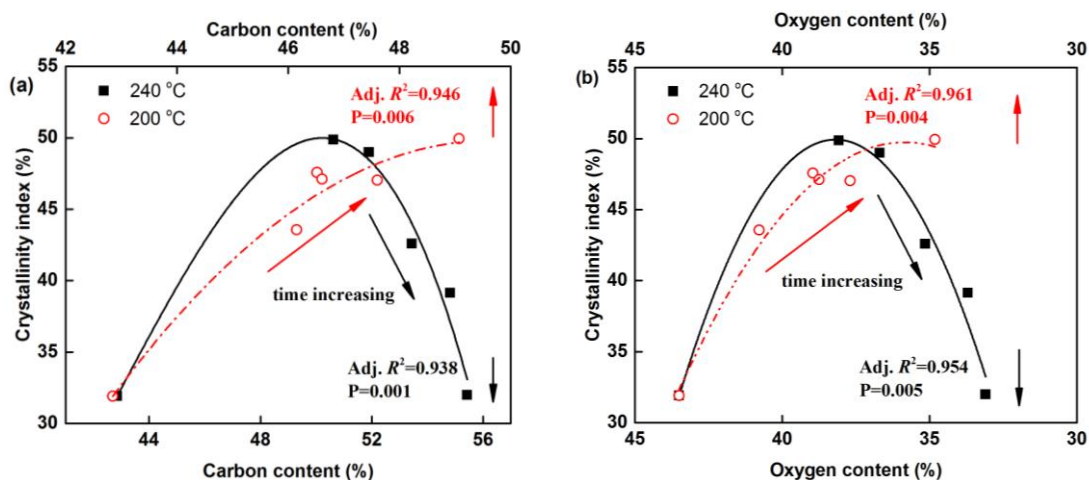
Fig. 7. Correlation between C/O Content and Crystallinity Index

Figure 8 depicts the FTIR spectra of untreated and hydrothermal treated samples. The wide band located at 3100 to 3700 cm^{-1} was associated with O–H vibration in hydroxyl or carboxyl groups. The bands located at 2921 and 2855 cm^{-1} were associated with aliphatic C–H stretching vibration and deforming vibration. The band at 1061 cm^{-1} was associated with the β-glycosidic bond in cellulose and hemicellulose (Liu *et al.* 2013). These bands were present both in the untreated sample and their HTC sample. However, compared with the untreated sample, some differences appeared after 30 min of HTC treatment at both temperatures. An absorption peak located at 1515 cm^{-1}, which could be related to aromatic ring stretching vibration appeared. This could be attributed to the removal of the amorphous fraction (Nitsos *et al.* 2013), as indicated in Fig. 7. The absorbance peak at 1700 cm^{-1} representing the C=O became stronger than the feedstock. This difference indicated that the chemical components of lawn grass started to degrade and simultaneously underwent the reaction of polymerization. However, band at 3100 to 3700 cm^{-1} of O-H vibration obviously decreased at 240 °C for 30 min, which might be caused by the dehydration reaction. At 240 °C, with increasing residence time, the absorbance intensity at 1700 cm^{-1} of C=O gradually increased. The band at 1030 to 1160

cm^{-1} associated with the cellulose (Liu *et al.* 2013) decreased over time, which was in agreement with XRD pattern.

After HTC treatment, lawn grass could be transformed into hydrochar with significantly increased HHV, increased carbon content, and decreased O/C and H/C ratios, especially at 240 °C, which provided potential application in some applications, such as co-combustion with other fossil fuel. However, the solid yield was relatively low. Recovery of liquid product should be considered in the application (Stemann *et al.* 2013).
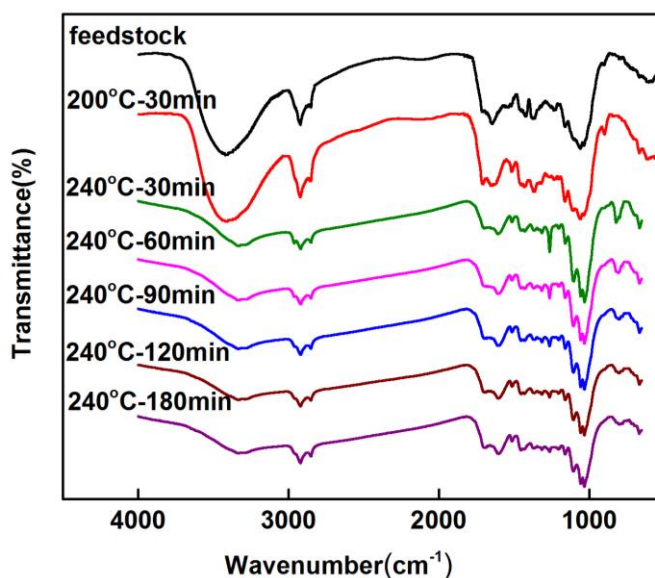
Fig. 8. FTIR spectra of feedstock and hydrochar at 200 and 240 °C

CONCLUSIONS

1. In the present study, lawn grass was converted to hydrochar by hydrothermal carbonization at 200 and 240 °C for 30 to 180 min. The mass yield of hydrochar varied from 50% at 200 °C for 30 min to 31% at 240 °C for 180 min. The C content and HHV of hydrochar increased from 42.9% and 17 MJ/kg (untreated) to 55.43% and 20.54 MJ/kg at 240 °C for 180 min, respectively. The hydrogen/carbon (H/C) and oxygen/carbon (O/C) atomic ratios of all solid residues were 1.17 to 1.64 and 0.45 to 0.65, respectively.

2. Temperature had the main influence on yield, carbon content, and HHV of hydrochar. Longer residence time was favorable for the dehydration, decarboxylation, and polymerization reactions, which resulted in carbon content increasing and oxygen content decreasing.

3. Based on X-ray diffraction, at a low temperature of 200 °C, with an increase of residence time from 30 to 180 min, the crystalline structure of hydrochar was gradually enhanced and the hydrochar production was mainly derived from the degradation of amorphous components. At the high temperature 240 °C, longer residence time promoted crystalline cellulose components in lawn grass to form hydrochar, so the peaks representing the crystalline cellulose became wider and

weaker and crystallinity index decreased. The FTIR spectra further confirmed the results of XRD pattern.

ACKNOWLEDGMENTS

REFERENCES CITED

Bobleter, O. (1994). "Hydrothermal degradation of polymers derived from plants," *Progress in Polymer Science* 19(5), 797-841. DOI: 10.1016/0079-6700(94)90033-7

Chen, D. Y., Zhou, J. B., Zhang, Q. S., Zhu, X. F., and Lu, Q. (2014). "Upgrading of rice husk by torrefaction and its influence on the fuel properties," *BioResources* 9(4), 5893-5905. DOI: 10.15376/biores.9.4.5893-5905

Funke, A., and Ziegler, F. (2010). "Hydrothermal carbonization of biomass: A summary and discussion of chemical mechanisms for process engineering," *Biofuels, Bioproducts & Biorefining* 4(2), 160-177. DOI: 10.1002/bbb.198

Gao, Y., Wang, X. H., Wang, J., Li, X. P., Cheng, J. J., Yang, H. P., and Chen, H. P. (2013). "Effect of residence time on chemical and structural properties of hydrochar obtained by hydrothermal carbonization of water hyacinth," *Energy* 58(1), 376-383. DOI: 1 0.1016/j.energy.2013.06.023

GB/T 28731 (2012). "Proximate analysis of solid biofuels," *Standardization Administration of the People's Republic of China*.

Hashaikeh, R., Fang, Z., Butler I. S., Hawari, J., and Kozinski, J. A. (2007). "Hydrothermal dissolution of willow in hot compressed water as a model for biomass conversion," *Fuel* 86(10-11), 1614-1622. DOI: 10.1016/j.fuel.2006.11.005

Kalyani, P., Ariharaputhiran, A., and Darchen, A. (2013). "Activated carbon from grass - A green alternative catalyst support for water electrolysis," *International Journal of Hydrogen Energy* 38(25), 10364-10372. DOI: 10.1016/j.ijhydene.2013.06.022

Kang, S. M., Li, X. L., Fan, J., and Chang, J. (2012). "Characterization of hydrochars produced by hydrothermal carbonization of lignin, cellulose, D-xylose, and wood meal." *Industrial & Engineering Chemistry* 51(26), 9023-9031. DOI: 10.1021/ie300565d

Li, G. Y., Huang, L. H., Hse, C. Y., and Qin, T. F. (2011). "Chemical compositions, infrared spectroscopy, and X-ray diffractometry study on brown-rotted woods," *Carbohydrate Polymers* 85(3), 560-564. DOI: 10.1016/j.carbpol.2011.03.014

Liu, S., Tian, J. Q., Wang, L., Zhang, Y. W., Qin, X. Y., Luo, Y. L., Asiri, A. M., Al-Youbi, A. O., and Sun, X. P. (2012). "Hydrothermal treatment of grass: A low-cost, green route to nitrogen-doped, carbon-rich, photoluminescent polymer nanodots as an effective fluorescent sensing platform for label-free detection of Cu(II) ions," *Advanced Materials* 24(15), 2037-2041. DOI: 10.1002/adma.201200164

Liu, Z. G., Quek, A., Hoekman, S. K., and Balasubramanian, R. (2013). "Production of solid biochar fuel from waste biomass by hydrothermal carbonization," *Fuel* 103, 943-949. DOI: 10.1016/j.fuel.2012.07.069

Lu, X. W., and Pellechia, P. J. (2013). "Influence of reaction time and temperature on product formation and characteristics associated with the hydrothermal carbonization of cellulose," *Bioresource Technology* 138, 180-190. DOI: 10.1016/j.biortech.2013.03.163

McEniry, J., Allen, E., Murphy, J. D., and Kiely, P. O. (2014). "Grass for biogas production: The impact of silage fermentation characteristics on methane yield in two contrasting biomethane potential test systems," *Renewable Energy* 63, 524-530. DOI: 10.1016/j.biortech.2014.07.007

Meyer, A. K. P., Ehimen, E. A., and Holm-Nielsen, J. B. (2014). "Bioenergy production from roadside grass: A case study of the feasibility of using roadside grass for biogas production in Denmark," *Resources, Conservation and Recycling* 20, 124-133. DOI: 10.1016/j.resconrec.2014.10.003

Nitsos, C. K., Matis, K. A., and Triantafyllidis, K. S. (2013). "Optimization of hydrothermal pretreatment of lignocellulosic biomass in the bioethanol production process," *ChemSusChem* 6(1), 110-120. DOI: 10.1002/cssc.201200546

Poerschmann, J., Weiner, B., Wedwitschka, H., Baskyr, I., Koehler, R., and Kopinke, F.-D. (2014). "Characterization of biocoals and dissolved organic matter phases obtained upon hydrothermal carbonization of brewer's spent grain," *Bioresource Technology* 164, 162-169. DOI: 10.1016/j.biortech.2014.04.052.

Reza, M. T., Lynam, J. G., Vasquez, V. R., and Coronella, C. J. (2013). "Hydrothermal carbonization: Fate of inorganics," *Biomass and Bioenergy* 49, 86-94. DOI: 10.1016/j.biombioe.2012.12.004

Reza, M. T., Wirth, B., Lüder, U., and Werner, M. (2014). "Behavior of selected hydrolyzed and dehydrated products during hydrothermal carbonization of biomass," *Bioresource Technology* 169, 352-361. DOI: 10.1016/j.biortech.2014.07.010

Roman, S., Nabais, J. M. V., Laginhas, C., Ledesma, B., and Gonzalez, J. F. (2012). "Hydrothermal carbonization as an effective way of densifying the energy content of biomass," *Fuel Processing Technology* 103, 78-83. DOI: 10.1016/j.fuproc.2011.11.009

Sevilla, M., Macia-Agullo, J. A., and Fuertes, A. B. (2011). "Hydrothermal carbonization of biomass as a route for the sequestration of CO_2: Chemical and structural properties of the carbonized products," *Biomass and Bioenergy* 35(7), 3152-3159. DOI: 10.1016/j.biombioe.2011.04.032

Steinbeiss, S., Gleixner, G., and Antonietti, M. (2009). "Effect of biochar amendment on soil carbon balance and soil microbial activity," *Soil Biology and Biochemistry* 41(6), 1301-1310. DOI: 10.1016/j.soilbio.2009.03.016

Stemann, J., Putschew, A., and Ziegler, F. (2013). "Hydrothermal carbonization: process water characterization and effects of water recirculation," *Bioresour. Technol.* 143, 139-146. DOI: 10.1016/j.biortech.2013.05.098

Wiedner, K., Rumpel, C., Steiner, C., Pozzi, A., Maas, R., and Glaser, B. (2013). "Chemical evaluation of chars produced by thermochemical conversion (gasification, pyrolysis and hydrothermal carbonization) of agro-industrial biomass on a commercial scale," *Biomass and Bioenergy* 59, 264-278. DOI: 10.1016/j.biombioe.2013.08.026

Xiao, L. P., Shi, Z. J., Xu, F., and Sun, R. C. (2012). "Hydrothermal carbonization of lignocellulosic biomass," *Bioresource Technology* 118, 619-623. DOI: 10.1016/j.biortech.2012.05.060

Yang, H. P., Yan, R., Chen, H. P., Zheng, C. G., Lee, D. H., and Liang, D. T. (2006). "In-depth investigation of biomass pyrolysis based on three major components: Hemicellulose, cellulose and lignin," *Energy & Fuels* 20(1), 388-393. DOI: 1 0.1021/ef0580117

Zhang, L. Y. (2003). "Analysis of conventional ingredients in feed," in: *Feed Analysis and Quality Monitoring Technique, 2nd Edition*, L. Y. Zhang (ed.), China Agricultural University Press, Beijing.

Zhang, L., Liu, S. S., Wang, B. B., Wang, Q., Yang, G. H., Chen, J. C. (2015). "Effect of residence time on hydrothermal carbonization of corn cob residual," *BioResources* 10(3), 3979-3986. DOI: 10.15376/biores.10.3.3979-3986